

## Supporting information for the paper

# **SPIO@SiO<sub>2</sub>-Re@PEG nanoparticles as magneto-optical dual probes and sensitizers for photodynamic therapy**

Marco Galli,<sup>#</sup> Elisa Moschini,<sup>◇</sup> Maria Vittoria Dozzi,<sup>#</sup> Paolo Arosio,<sup>‡&</sup> Monica Panigati,<sup># & ¥</sup> Laura D'Alfonso,<sup>§</sup> Paride Mantecca,<sup>◇</sup> Alessandro Lascialfari,<sup>‡&</sup> Giuseppe D'Alfonso,<sup>#&</sup> and Daniela Maggioni<sup>\* #&</sup>

<sup>#</sup> Dipartimento di Chimica, Università degli Studi di Milano, Via Golgi 19, 20133 Milano, Italy

<sup>◇</sup> Dipartimento di Scienze dell'Ambiente e del Territorio e di Scienze della Terra, Università di Milano Bicocca, Piazza della Scienza 3, 20126 Milano, Italy

<sup>‡</sup> Dipartimento di Fisica, Università degli Studi di Milano, Via Celoria 16, 20133 Milano, Italy

<sup>§</sup> Dipartimento di Fisica, Università di Milano Bicocca, Piazza della Scienza 3, 20126 Milano, Italy

<sup>&</sup> Consorzio Interuniversitario Nazionale per la Scienza e Tecnologia dei Materiali, Via Golgi 19, 20133 Milano, Italy

<sup>¥</sup> Istituto per lo Studio delle Macromolecole, Consiglio Nazionale delle Ricerche (ISMAR-CNR), Via E. Bassini, 15, 20133 Milano, Italy

## Experimental details.

**S.1. Materials.** Oleic acid (OA, 90% technical grade, Alfa Aesar), 1-octadecene (99%, Sigma-Aldrich), methanol (99.8%, Sigma-Aldrich), ethanol (99.8%, Sigma-Aldrich), 3-(triethoxysilyl)propyl isocyanate (95% Sigma-Aldrich), 4-aminopyridine (98%, Fluka), pyridine (99.5%, LAB-SCAN Analytical Sciences), TEOS (tetraethoxysilane, >99%, Aldrich), 1,5-dihydroxynaphthalene (DHN, Aldrich, 97%), 1,10-phenanthroline monohydrate (99.5%, Merck), PEG<sub>500</sub> monomethylether (Sigma-Aldrich), IGEPAL CO-520 (Sigma-Aldrich), diethylether (99.8%, Sigma-Aldrich), dichloromethane (99.9%, Sigma-Aldrich), n-hexane (96%, Scharlau), cyclohexane (99.5% LAB-SCAN Analytical Sciences), toluene (99.7%, Sigma-Aldrich), NH<sub>3</sub> (28%, VWR), HCl (30% suprapur, Merck), HF (48%, Merck), HNO<sub>3</sub> (65% suprapur, Merck) H<sub>2</sub>O<sub>2</sub> (30% suprapur, Merck), Methylene Blue hydrate (Sigma-Aldrich), Re<sub>2</sub>(CO)<sub>10</sub> (99.99%, Acros organics), anhydrous FeCl<sub>3</sub> (99%, Fluka), silver triflate (99%, Sigma-Aldrich), OptiMEM (Thermo Fischer), Foetal Bovine Serum (Thermo Fischer), Hoechst 33342 (Sigma-Aldrich), 3-(4,5-Dimethyl-2-thiazolyl)-2,5-diphenyl-2H-tetrazolium bromide-MTT (Sigma-Aldrich), were used as received if not otherwise specified.

**S.2. Instruments and Methods.** High resolution NMR experiments were performed on a Bruker Model DRX400 spectrometer (operating at 400.13 and 100.62 MHz for <sup>1</sup>H and <sup>13</sup>C NMR, respectively), equipped with a Bruker 5 mm BBI Z-gradient probe head capable of producing gradients with a strength of 53.5 G/cm.

Infrared (IR) spectra were acquired on a Bruker Model Vector 22 FT instrument, using 0.1 mm CaF<sub>2</sub> cells.

Photophysical measurements were carried out in air-equilibrated water solutions at 298 K. Electronic absorption spectra were recorded on an Agilent Model 8543 spectrophotometer at room temperature and using quartz cells with 1.0 cm path length. A Jasco V-650 spectrophotometer was employed to monitor the progress of the photosensitization reactions.

Emission spectra were obtained with an Edinburgh FLS980 spectrofluorometer equipped with a

450 W xenon arc lamp. Emission spectra were corrected for source intensity (lamp and grating) and emission spectral response (detector and grating) by standard correction curves. Photoluminescence quantum yields were measured with a Hamamatsu Photonics absolute PL quantum yield measurement system (C11347-01 Quantaaurus spectrometer) equipped with a L11562 Xenon light source (150 W), monochromator, C7473 photonic multi-channel analyzer, integrating sphere and employing U6039-05 PLQY measurement software (Hamamatsu Photonics, Ltd., Shizuoka, Japan).

Luminescent excited state lifetimes in the range from 0.5 ns to 5  $\mu$ s were measured by an Edinburgh FLS980 spectrofluorometer equipped with a TCC900 card for data acquisition in time-correlated single-photon counting experiments (0.2 ns time resolution) with a 375 nm pulsed diode. The estimated experimental errors are 2 nm on the absorption and PL bands maxima, 5% on the molar absorption coefficient, and on the luminescence quantum yield.

Metal content on NPs was determined by ICP analysis on a Perkin–Elmer Optima 8300 instrument or by AAS analysis on a Perkin-Elmer Pinaacle 900 instrument.

DLS and  $\zeta$ -potential measurements were carried out on a Zetasizer Nano ZS instrument (Malvern Instruments Corp., Malvern, Worcestershire, UK) at a wavelength of 633 nm with a solid state He–Ne laser at a scattering angle of 173°, at 298 K on diluted samples at pH 7. Each hydrodynamic diameter was averaged from at least three measurements.

Transmission electron microscopy (TEM) images were collected using a EFTEM LEO 912AB (Zeiss). The samples suspended in water were deposited by drop casting onto copper grids (Cu-300 CK, 300 mesh), and left to naturally go to dryness for one night. The statistics has been obtained using the free software Image-J 1.48v.

For nuclear magnetic resonance (NMR) relaxometry, the NMR signal detection and generation was obtained with a Smartracer® Fast-Field-Cycling relaxometer (Stelar, Mede, Italy) in the range 10 kHz–10 MHz and with a Stelar Spin-master spectrometer in the 10 MHz–60 MHz range. In the second case, standard radio frequency excitation sequences were used for T1 and T2 measurements, respectively saturation-recovery for T1, Carr Purcell Meiboom Gill (CPMG) for T2. For the very

low field range ( $\nu < 4$  MHz for T1 and  $\nu < 3.5$  MHz for T2 ), ad hoc pre-polarized sequences were used to increase the NMR proton signal.<sup>1,2</sup> Relaxation data were analyzed by means of the Stelar Company (Mede, Italy) software or homemade software, and Origin (Microcal).

The photochemical experiments were performed in a 3 mL quartz cuvette, inserted in a home made housing consisting in a black box mounted on optical bench. The irradiation source was an Osram, model Powerstar HCI-T, 150 W/NDL lamp, mounted on a Twin Beam T 150 R reflector, mainly emitting visible light above 400 nm, with a small emission in the 350–400 nm range which was eliminated after the location of a 390 nm cut off filter at the black box entrance (Fig. S1). The lamp and the reactor were separated by a fixed distance of 10 cm. The whole set up was maintained at ambient temperature by a continuous stream of air.

Two photon excitation (TPE) confocal microscopy measurements on A549 cells were performed by an optical setup built around a confocal scanning head (FV-300, Olympus, Japan) mounted on an upright optical microscope (BX51, Olympus, Japan) equipped with a high working distance objective (NA = 1.1, wd = 2 mm, 60X, water immersion, Olympus, Japan). TPE imaging was performed through the FV-300 scanning unit after removing the largest pinhole from the pinhole wheel. The objective simultaneously focused the laser beam on the sample and collected the signal in epi-fluorescence geometry through the non-descanned collection channels described elsewhere.<sup>3</sup> The fluorescence signal was filtered by a 485/50, a 535/50 and a 600/40 band-pass filter in order to select the fluorescence light and remove either scattering or undesired auto-fluorescence from the sample, and it was processed by means of the Fluoview 5.0 software (Olympus, Japan). The laser source was a mode-locked Ti:sapphire laser (Mai Tai HP, Spectra Physics, CA) with pulses of 120 fs full width at half maximum and 80 MHz repetition frequency. The bleed through of autofluorescence was verified on non-stained samples by measuring the fluorescence emission in the presence and in the absence of the band pass filter selecting the emission of the samples. Images shown in the paper are the result of 2 kalman average scans with 5  $\mu$ s of residence time per pixel. The field of view of the 1024x1024 pixel images was 79x79  $\mu$ m<sup>2</sup>.

For the cell viability, assessed by MTT, the optical density of the samples was measured with a multiplate reader Multiskan Ascent (Thermo Electron Corporation, Vantaa, Finland).

**S.3. Synthesis of SPIO@OA NPs.** The synthesis of magnetic nanoparticles was performed following a literature procedure.<sup>4</sup> Briefly, 1.48 g of Fe(OA)<sub>3</sub> (OA = oleic acid,  $1.6 \times 10^{-3}$  mol) freshly prepared from sodium oleate and FeCl<sub>3</sub> were dissolved in 10.3 mL of 1-octadecene and added with 260  $\mu$ L of oleic acid (ratio Fe(OA)<sub>3</sub>/OA = 5.70) under nitrogen. The mixture was heated at 3.3 °C/min from room temperature to 320 °C and left at this temperature for 30 min. Then, the mixture was left to come back to room temperature. The brownish red color turned to deep dark brown at the end of the heating cycle. The suspension was then treated with an excess of ethanol (1:3) and centrifuged (15 min at 7550 g), repeating the washing procedure for three times. Finally, the NPs were re-suspended in 15 mL of n-hexane and stored at -20 °C under nitrogen. [Fe] from AAS =  $6.45 \times 10^{-2}$  M, corresponding to 5 mg/mL SPIO NPs. Hydrodynamic diameter from DLS =  $10.4 \pm 1.3$  nm, diameter from TEM =  $9.5 \pm 0.9$  nm.

**S.4. Synthesis of the py-upts ligand.** Glassware was anhydriified beforehand, and pyridine used as solvent was distilled just before use. In a Schlenk tube under nitrogen, 4-aminopyridine (0.300 g, 3.13 mmol) and triethoxysilylpropylisocyanate (0.976 g, 3.95 mmol, 1.2 equiv) were dissolved in 12.5 mL of anhydrous pyridine, giving rise to a pale yellow solution. The mixture was heated at 60 °C and stirred for 48 h, then pyridine was evaporated under vacuum, and the sticky beige solid was repeatedly washed with anhydrous Et<sub>2</sub>O and evaporated under vacuum to remove the traces of the remaining pyridine. Yield 85%. <sup>1</sup>H NMR (400 MHz, DMSO-d<sub>6</sub>):  $\delta$  8.84 (s, 1H, NHCO), 8.27 (m, 2H, CH), 7.35 (m, 2H, CH), 6.40 (t,  $J = 5.7$  Hz, 1H, NHCO), 3.75 (quart,  $J = 6.9$  Hz, 2H, CH<sub>2</sub>), 3.08 (quart,  $J = 6.6$  Hz, 2H, CH<sub>2</sub>), 1.49 (m, 2H, CH<sub>2</sub>), 1.15 (t,  $J = 6.9$  Hz, 3H, CH<sub>3</sub>), 0.59 (m, 2H, CH<sub>2</sub>).

**S.5. Synthesis of PEG<sub>500</sub>-Silane (N-(3-triethoxysilyl)propyl-O-PEG(OMe)-carbamate) ligand.** The functionalization of PEG monomethylether was performed by a slightly modified

literature procedure.<sup>5</sup> In a two necked flask a sample of PEG<sub>500</sub> monomethylether (1 g, 2 mmol) was dissolved in 25 mL of anhydrous toluene under nitrogen, together with 3-(triethoxysilyl)propyl isocyanate (625  $\mu$ L, 2.5 mmol). The solution was then heated to 85 °C for 24 h. The reaction was monitored through FTIR spectroscopy, by following the appearance of the carbamate band (at 1728  $\text{cm}^{-1}$ ) and the concomitant decrease of the isocyanate band (at 2272  $\text{cm}^{-1}$ ). The toluene solution was evaporated under reduced pressure. The residue was dissolved in  $\text{CH}_2\text{Cl}_2$  and precipitated as white solid by addition of n-hexane. The crude precipitate of PEG<sub>500</sub>-silane was washed for three times with few mL of n-hexane to separate all the unreacted 3-(triethoxysilyl)propyl isocyanate. Finally PEG<sub>500</sub>-silane was dried under reduced pressure in vacuum. <sup>1</sup>H NMR (400 MHz,  $\text{CDCl}_3$ )  $\delta$  5.02 (br m,  $\text{NHCOO}$ , 1H), 4.22 (t,  $J = 4.4$  Hz, 2H,  $\text{CH}_2$ ), 3.83 (quart,  $J = 7.03$  Hz 6H,  $\text{CH}_2$ ), 3.66 (*pseudo* s,  $\text{CH}_2\text{CH}_2\text{O}$  PEG chain), 3.40 (s, 3H,  $\text{OCH}_3$ ), 3.18 (q,  $J = 3.2$  Hz, 2H,  $\text{CH}_2$ ), 1.63 (*pseudo* q,  $J_{\text{app}} = 7.5$  Hz, 2H,  $\text{CH}_2$ ), 1.24 (t,  $J = 7.03$  Hz 9H,  $\text{CH}_3$ ), 0.58 (m, 2H,  $\text{CH}_2$ ).

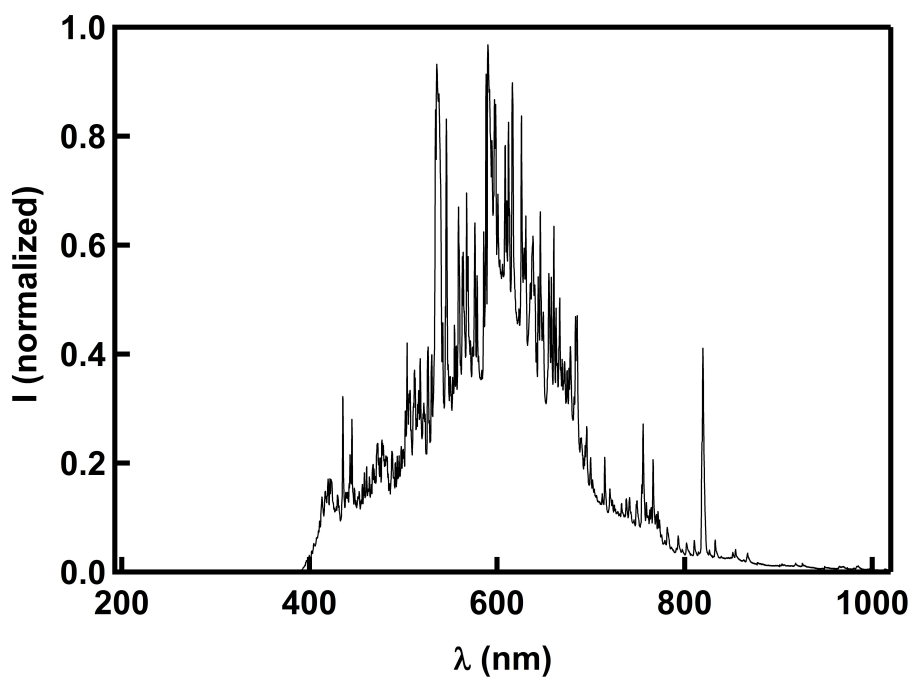


**Figure S1.** Emission spectrum of the lamp used for the photochemical production of  $^1\text{O}_2$ , both in cuvette and in multi well plates on A549 cells (Osram, model Powerstar HCI-T, 150 W/NDL).

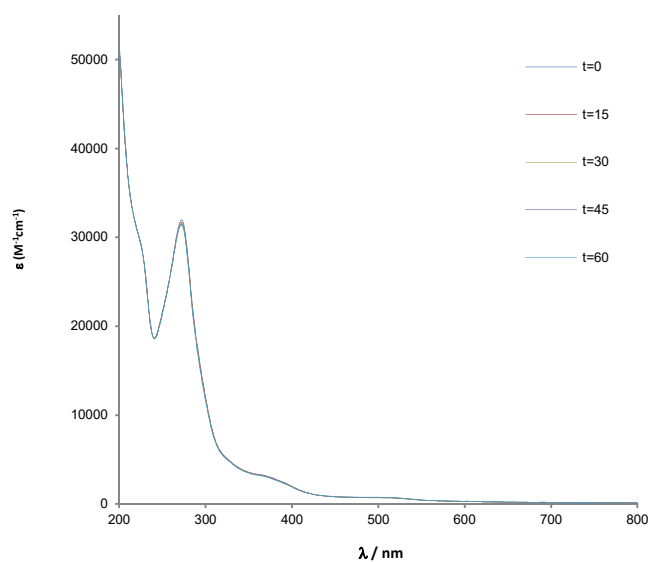


**Figure S2.** Photochemical stability test: UV-vis absorption spectra at different irradiation times (numbers in the legend indicate minutes) of a water solution of  $[\text{Re}(\text{phen})(\text{CO})_3(\text{py-upts})]\text{OTf}$  ( $1.3 \times 10^{-5}$  M) saturated with  $\text{O}_2$ .

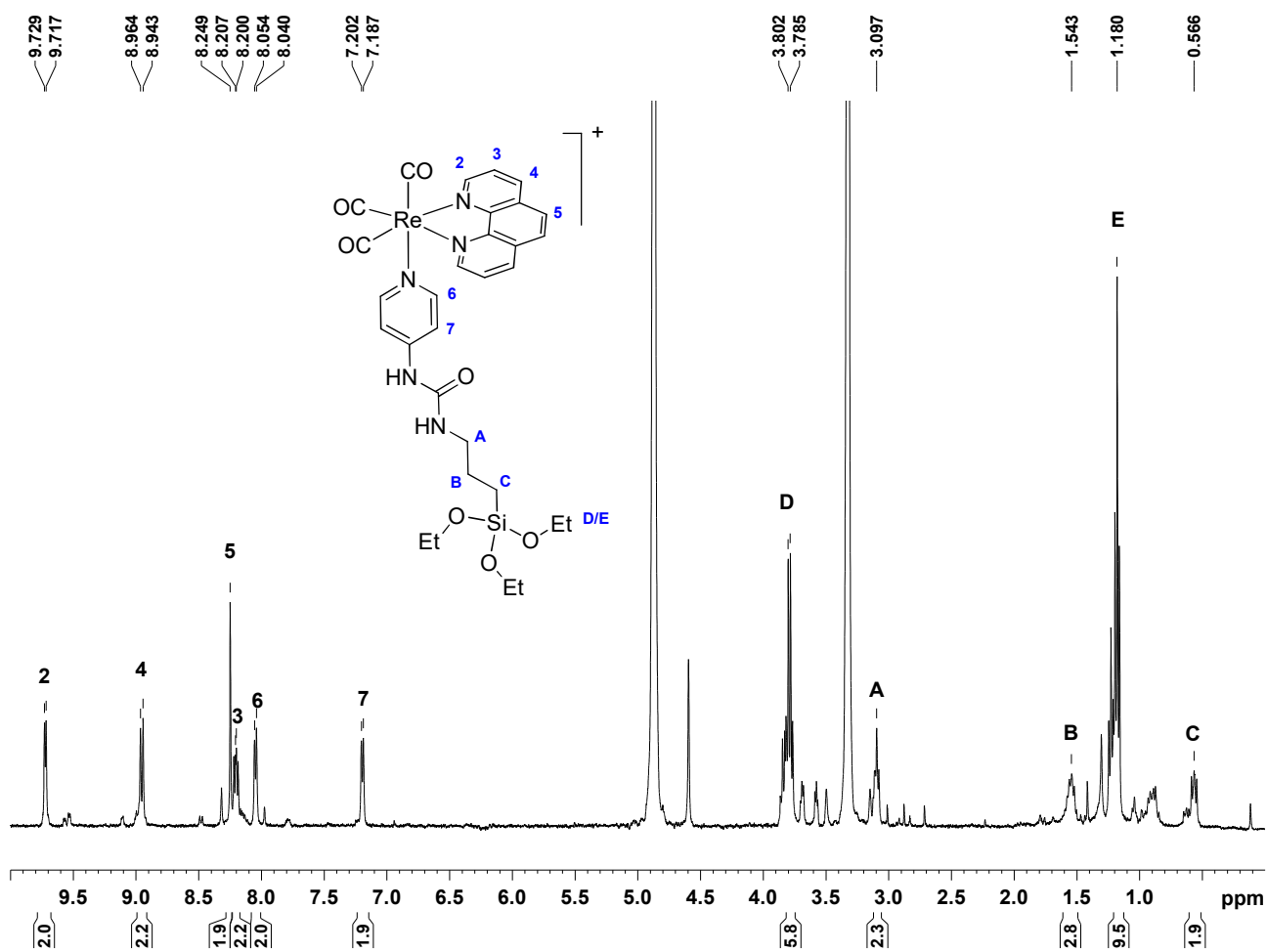


**Figure S3.**  $^1\text{H}$  NMR spectrum for the monitoring of the reaction of  $[\text{Re}(\text{phen})(\text{CO})_3\text{OTf}]$  with py-upts to give the complex  $[\text{Re}(\text{phen})(\text{CO})_3(\text{py-upts})]\text{OTf}$  (300 K, MeOD, 9.7 T). The minor peaks are due to the starting reagents.



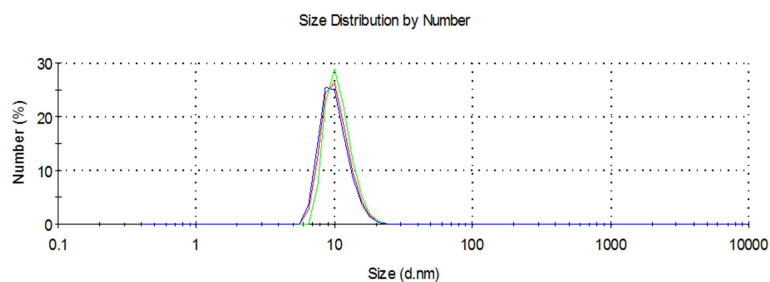


**Figure S4.** DLS size distribution by numbers of a diluted sample of SPIO@OA.

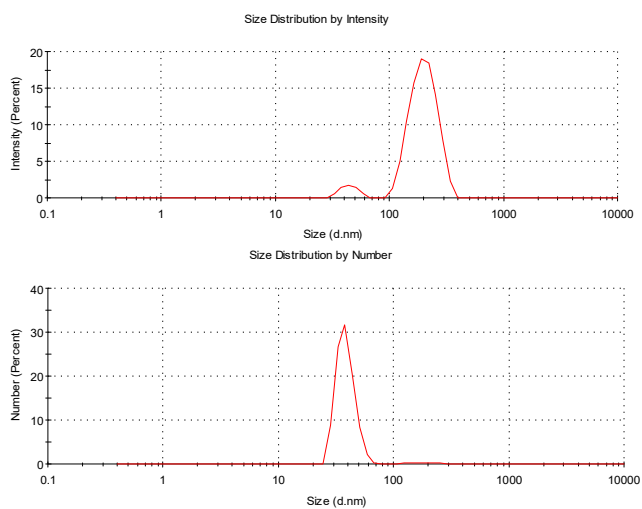


**Figure S5.** DLS size distribution by intensities and by numbers of a diluted sample of SPIO@SiO<sub>2</sub> NPs suspended in water. The number size distribution indicates that the population with the largest size (and then the highest scattering power) is negligible with respect to the smaller one.

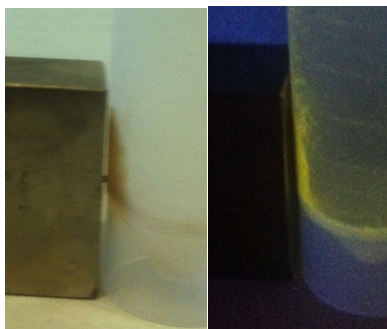


**Figure S6.** Digital photographs of an aqueous suspension of SPIO@SiO<sub>2</sub>-Re@PEG NPs nearby a permanent magnet, observed under solar light (left) and UV lamp (right).

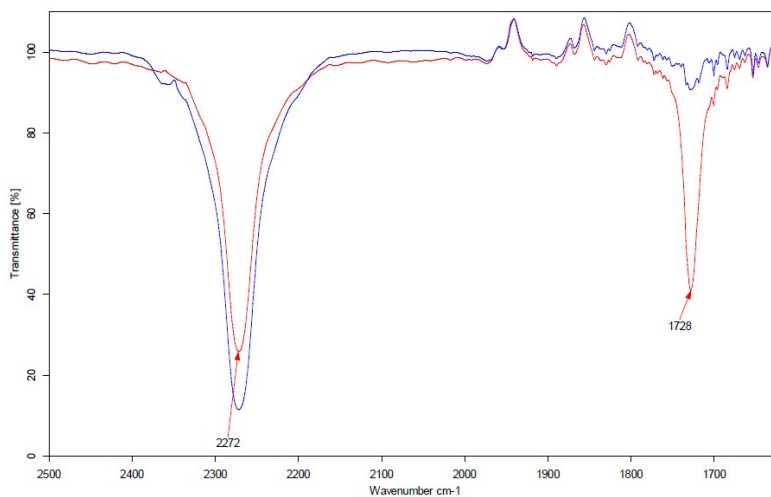


**Figure S7.** FTIR spectra (carbonyl region) of the isocyanate-triethoxysilane molecule, showing the isocyanate CO stretching at 2272 cm<sup>-1</sup> (blue trace), and of the mixture of reaction with PEG<sub>500</sub> monomethylether, showing the formation of the carbamate link (red trace, carbamate CO stretching at 1728 cm<sup>-1</sup>).

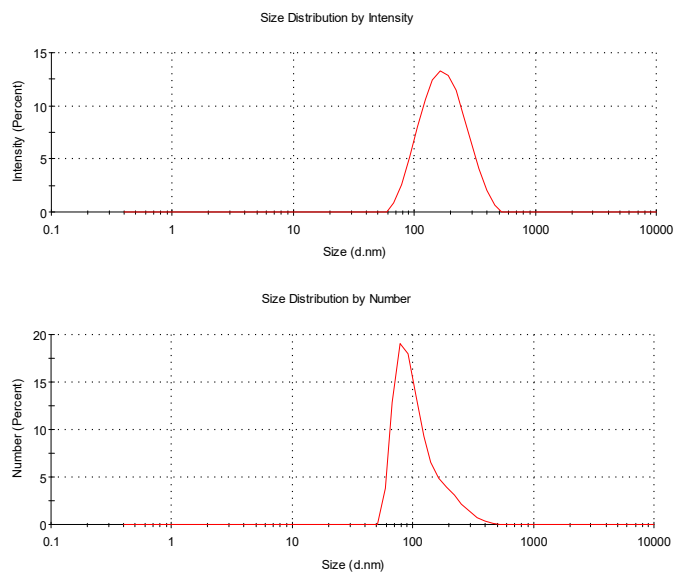


**Figure S8.** DLS size distribution by intensities and by numbers of a diluted sample of SPIO@SiO<sub>2</sub>-Re@PEG NPs suspended in water.

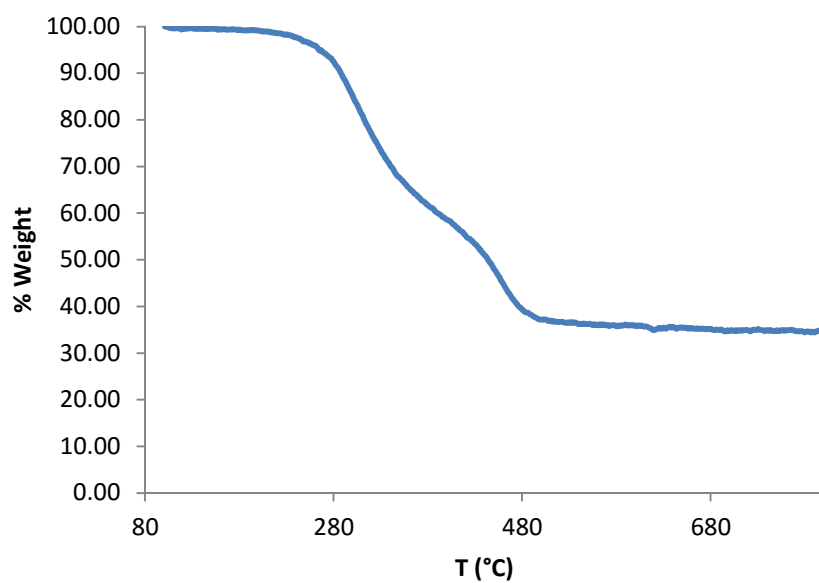


**Figure S9.** Thermogravimetric analysis of a dried sample of SPIO@SiO<sub>2</sub>-Re@PEG NPs.

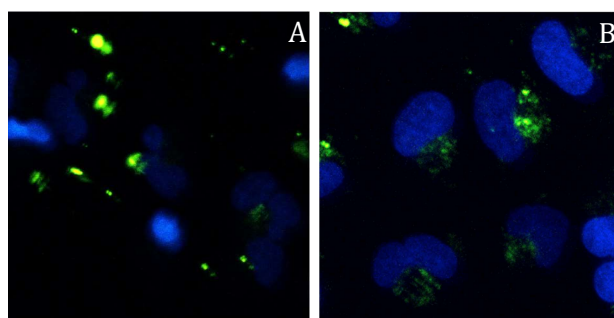


**Figure S10.** TPE microscopy images of A549 cells exposed to  $[\text{Re}(\text{phen})(\text{CO})_3(\text{py-upts})]\text{OTf}$ , result of the projection and superposition on the xy plane of 10 single planes acquired along the z axis at  $0.5 \mu\text{m}$  steps, after 4 h (panel A) and 24 h (panel B) of incubation.

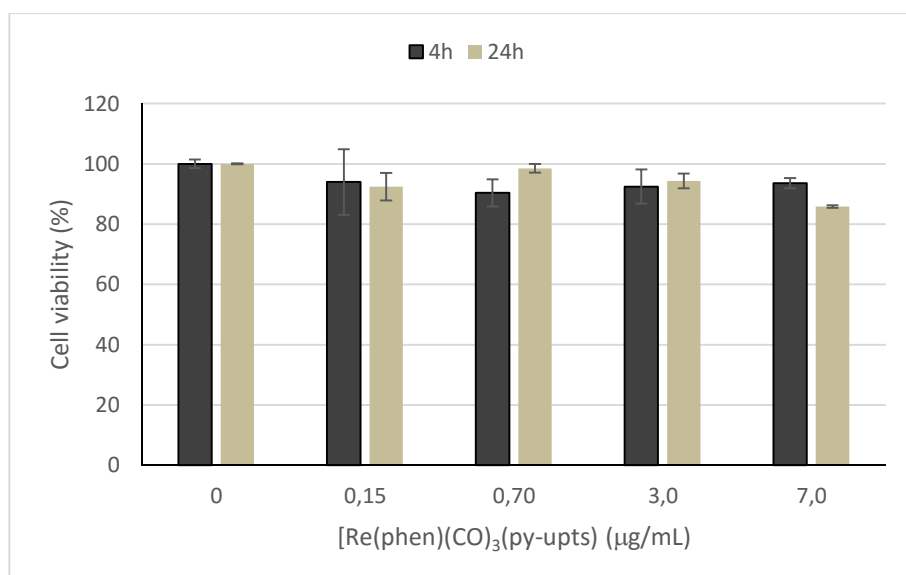


**Figure S11.** Cell viability results (MTT) after incubation of A549 cells for 4 h and 24 h with the free complex  $[\text{Re}(\text{phen})(\text{CO})_3(\text{py-upts})]\text{OTf}$ .

## References

---

- <sup>1</sup> R. Kimmich, E. Ansaldo, *Prog. Nucl. Magn. Reson. Spectrosc.*, 2004, **44**, 257–320.
- <sup>2</sup> G. Ferrante, S. Sykora, *Adv. Inorg. Chem.*, 2005, **57**, 405–470.
- <sup>3</sup> D. Maggioni, M. Galli, L. D'Alfonso, D. Inverso, M. V. Dozzi, L. Sironi, M. Iannaccone, M. Collini, P. Ferruti, E. Ranucci, G. D'Alfonso, *Inorg. Chem.*, 2015, **54**, 544–553.
- <sup>4</sup> J. Park, K. An, Y. Hwang, J.-G. Park, H.-J. Noh, J.-Y. Kim, J.-H. Park, N.-M. Hwang, T. Hyeon, *Nat. Mater.*, 2004, **3**, 891–895.
- <sup>5</sup> B. Radi, R. M. Wellard, G. A. George, *Soft Matter*, 2013, **9**, 3262–3271.